High Resolution Compressed Sensing Radar using Difference Set Codes

Iman Taghavi, Mohamad F. Sabahi, Farzad Parvaresh and Mohsen Mivehchy

arXiv:1605.05379v1 [cs.IT] 17 May 2016

***Abstract*—In this paper, we consider compressive sensing (CS)-based recovery of delays and Doppler frequencies of targets in high resolution radars. We propose a novel sub-Nyquist sampling method in the Fourier domain based on difference sets (DS), called DS-sampling, to create dictionaries with highly incoherent atoms. The coherence of the dictionary reaches the Welch minimum bound if the DS-sampling is employed. This property let us to implement sub-Nyquist high resolution radars with minimum number of samples[1]. We also develop a low complexity recovery method, based on structured CS and propose a new waveform, called difference set–frequency coded modulated (DS-FCM) waveform, to boost the recovery performance of the sub-Nyquist radar in noisy environments. The proposed method solves some of the common problems in many CS-based radars and overcome disadvantages of the conventional Nyquist processing, *i.e.* matched filtering in high resolution radar systems. The proposed method allows us to design sub-Nyquist radars, which require less than 2% of Nyquist samples and recover targets without resolution degradation in comparison to the conventional Nyquist processing.**

***Index Terms*—Compressive sensing (CS), difference set (DS), Welch bound, coherence, structured CS, Doppler focusing, high resolution radar.**

I. Introduction

Matched filtering and fast Fourier transform (FFT) are the two conventional processing techniques used in monostatic pulse-Doppler radars, which are employed to estimate delays and Doppler frequencies of targets, respectively. In the conventional processing, the delay and Doppler resolution of a radar relatively depend on the bandwidth of the radar waveform and the number of pulses that the radar transmits and receives from the targets [1]. Hence, high resolution radar systems use waveforms with large bandwidth, and according to the Shannon-Nyquist theorem [2], these radars require to sample the received signals in the radars receivers at high rates. Another disadvantage of matched filtering in the radars receivers is producing relatively large side-lobes for stronger targets, which may cover nearby weaker ones [1]. In this paper, we propose a novel sub-Nyquist sampling scheme for the radar receiver, which relaxes the dependency of the sampling rate in the radar receiver to the radar waveform bandwidth and consequently the radar resolution.

The authors are with the Department of Electrical Engineering, University of Isfahan, Isfahan, Iran (e-mail: i.taghavi.ir@ieee.org, sabahi@eng.ui.ac.ir, f.parvaresh@eng.ui.ac.ir, mivehchy@eng.ui.ac.ir).

[1]Notice that for an optimal sub-Nyquist radar we expect that the number of samples to be $K = O(S \log^c N/S)$, where S is the number of targets and N is the number of Nyquist samples. However, for a dictionary construction based on the coherence, one can show that for successful recovery $K = O(S^2)$, and our construction, in this sense, is optimal.

Compressed sensing or compressive sampling (CS), which rigorously was firstly studied by Donoho [3] and Candes *et. al.* [4], is an emerging field that has attracted considerable amount of research over the past decade. One of the main goals of CS is sampling wideband signals with *known properties*, such as sparsity, at rates significantly lower than the Shannon-Nyquist rate without losing the information that is required to reconstruct the signals from the samples. In practice, sampling a signal at a sub-Nyquist rate means that a lower rate analog to digital converters (ADCs) is required, which leads to less power consumption, heat dissipation and cost in the receiver circuit. Moreover, sampling at sub-Nyquist rate requires less memory for data processing [5], [6].

Several previous works study CS-based radar systems. The sparse estimation methods in [7] and [8] require a huge dictionary-size proportional to the product of the delay and Doppler grid sizes. The large dictionary-size in CS-based radar systems increases the computational complexity of the recovery algorithms and makes them infeasible for real-time target detection in CS-based radars. In [9], the authors propose a CS recovery algorithm for high resolution estimation of delays and Doppler frequencies, however, this work does not address the sample rate reduction. The authors of [10] have used recovery algorithms based on spectral estimation tools to recover delays and Doppler frequencies directly from the low rate samples. Finally, the recently proposed approach in [11], called Doppler focusing, uses a low complexity and robust algorithm to estimate delays and Doppler frequencies of targets. It is worth mentioning that the sub-Nyquist rate sampling schemes used in [10] and [11] degrade the delay resolution of radar compared to the conventional Nyquist processing radars.

In this paper, we focus on designing an optimal CS-dictionary and finding a low complexity recovery method for detecting targets in high resolution radars. We also introduce an appropriate radar waveform for this recovery algorithm.

Our contributions are as follows:

- A low complexity structured CS model and an efficient recovery algorithm for a high resolution radar with sub-Nyquist sampling is introduced.
- An optimal sub-Nyquist sampling technique based on difference sets called DS-sampling is proposed, which guarantees high resolution recovery of radar targets using CS algorithms.
- A frequency coded modulated waveform based on difference sets called DS-FCM waveform is presented, which improves the recovery performance of the CS-based radar significantly in noisy conditions.

- A modified version of the Doppler focusing (modified-DF) approach [11], based on the DS-sampling and DS-FCM waveform, is developed to increase resolution of Doppler focusing approach and make it more robust in noisy conditions.

Difference sets are well studied in combinatorics [12], [13]. Difference set codes have various applications in sequence design [12], communication systems [14], [15], array sensors [16], [17] and error correction systems [18]. The main idea of our work comes from [19], which uses difference sets to design complex code-books that achieve the Welch bound with equality.

The rest of the paper is organized as follows: In Section II, we describe the radar measurement models. We explain the properties of the sampling dictionary in Section III, we prove that highly incoherent dictionaries may be obtained via DS-sampling. The recovery algorithms for the proposed structured model is developed in Section IV. We introduce DS-FCM waveform in Section V. In Section VI we present the simulation results, and finally, we conclude the paper in Section VII.

Throughout the paper, we use the following notation. Matrices and vectors are denoted by bold letters, where we use lowercase letters, such as $\mathbf{x}$, for vectors and uppercase letters, such as $\mathbf{X}$, for matrices. The i^{th} element of a vector $\mathbf{x}$ is denoted by x_i and X_{ij} denotes the element in the matrix $\mathbf{X}$ that is in the i^{th} row and j^{th} column. The i^{th} column of the matrix $\mathbf{X}$ is denoted by the vector $\mathbf{x}_i$. Also, we use the notation $\tilde{\mathbf{x}}_i$ to denote the i^{th} column of the matrix $\mathbf{X}^T$, *i.e.* the transpose of the i^{th} row of the matrix $\mathbf{X}$. The cardinality of a set $\mathcal{K}$ is denoted by $|\mathcal{K}|$. $\mathbb{Z}_N = \{0, 1, ..., N-1\}$ denotes the set of integers modulo N. The l_p norm of a vector $\mathbf{x}$ with length n for $p \in [1, \infty)$ is defined as $\|\mathbf{x}\|_p = (\sum_{i=1}^{n} |\mathbf{x}_i|^p)^{\frac{1}{p}}$. The $\mathrm{rect}(\cdot)$ function represents a square pulse signal with height and width equal to one. Mathematically, $\mathrm{rect}(x) = 1$ if $|x| \leqslant 1/2$ and $\mathrm{rect}(x) = 0$ otherwise.

II. Radar Measurement Models

The transmitted signal of a radar is assumed to be a train of P pulses with pulse repetition interval (PRI) of τ

$$x_T(t) = \sum_{p=0}^{P-1} h(t - p\tau), \quad 0 \leqslant t < P\tau, \tag{1}$$

where $h(t)$ is a baseband pulse with the continuous-time Fourier transform (CTFT) $H(\omega)$ and two-sided spectrum bandwidth of B_h.

The common assumption in the radar signal processing is that the unknown parameters of targets (*i.e.* attenuation factors, delays and Doppler frequencies) are approximately remain constant during transmitting and receiving the P pulses, so this time interval is called the coherent processing interval (CPI) of the radar [1]. Based on this assumption, the received signal can be written as

$$y_R(t) = \sum_{p=0}^{P-1} \sum_{s=1}^{S} a_s \, h(t - t_s - p\tau) \, e^{j2\pi f_s t}, \tag{2}$$

where S is the number of targets and $\{a_s, t_s, f_s\}_{s=1}^{S}$ are unknown attenuation factors, delays and Doppler frequencies of the targets, respectively. Furthermore, we assume that the delays and Doppler frequencies belong to the unambiguous delay-Doppler region of the radar, meaning that $t_s \in [0, \tau)$ and $f_s \in [-1/2\tau, 1/2\tau)$ for $s = 1, 2, \ldots, S$.

Fourier coefficients of the received signal in the p^{th} PRI are

$$\begin{aligned} Y_p[k] &= \frac{1}{\tau} \int_0^{\tau} \sum_{s=1}^{S} a_s \, h(t - t_s) \, e^{j2\pi f_s (t + p\tau)} \, e^{-j\omega_k t} \, \mathrm{d}t \\ &= \frac{1}{\tau} \sum_{s=1}^{S} a_s e^{j2\pi f_s (t_s + p\tau)} \int_0^{\tau} h(t - t_s) e^{j2\pi f_s (t - t_s)} e^{-j\omega_k t} \, \mathrm{d}t, \end{aligned} \tag{3}$$

where $\omega_k = 2\pi k/\tau$ and the indices k are integers that belong to $\mathbb{Z}$. Using the time and frequency shifting properties of the Fourier transform we may rewrite (3) as

$$Y_p[k] = \frac{1}{\tau} \sum_{s=1}^{S} a_s \, H(\omega_k - 2\pi f_s) \, e^{j2\pi f_s p\tau} \, e^{-j(\omega_k - 2\pi f_s) t_s}. \tag{4}$$

Bandwidth of the radar waveform is typically much greater than the Doppler frequencies of targets. This implies that for most $k \in \mathbb{Z}$ we have $\omega_k \gg 2\pi f_s$. Using this fact we may approximate (4) by

$$Y_p[k] \approx \frac{1}{\tau} H(\omega_k) \sum_{s=1}^{S} a_s \, e^{j2\pi f_s p\tau} \, e^{-j\omega_k t_s}. \tag{5}$$

The approximation for the Fourier coefficients of the received signal, given in (5), is known as the Fourier coefficient of a semi-periodic finite rate of innovation (FRI) signal in the CS literature [5], and it has been used for radar signal modeling in previous works [10], [11].

Note that the radar waveform is a baseband pulse with the two-sided bandwidth of B_h. Therefore, assuming that the waveform has a symmetric spectrum, only the Fourier coefficients with indices k belonging to the set

$$\mathcal{I} = \left\{ -\left\lceil \frac{\tau B_h}{2} \right\rceil, \ldots, -1, 0, 1, \ldots, \left\lfloor \frac{\tau B_h}{2} \right\rfloor \right\}, \tag{6}$$

have non-zero values. Using this fact, we can give an interpretation of the Shannon-Nyquist theorem in the Fourier domain; We can reconstruct the received signal exactly, using $|\mathcal{I}| = \lceil \tau B_h \rceil$ Fourier coefficients per PRI. Commonly, B_h (related to both the positive and negative frequencies of $h(t)$) is called the *Nyquist frequency* or the *Nyquist rate* of the signal. In practice, we know that the targets are small objects in the space that is scanned by the radar. Thus, if we represent the pair of unknown delays and Doppler frequencies of all targets with points $\{(t_s, f_s)\}_{s=1}^{S}$, then, these points are distributed sparsely over the unambiguous delay-Doppler plane of the radar. CS theory predicts that high dimensional *sparse* signals can be recovered from highly incomplete measurements using efficient algorithms [4]. So, it is very promising to employ CS theory in order to recover sparse targets directly from sub-Nyquist samples.

The first step in the receiver of a CS-based radar is sampling the received signal with a rate that is far lower than the Nyquist rate. For this reason, we only acquire the Fourier coefficients in (5) for indices $k \in \mathcal{K} \subset \mathcal{I}$ such that $|\mathcal{K}| \ll |\mathcal{I}|$. For simplicity,

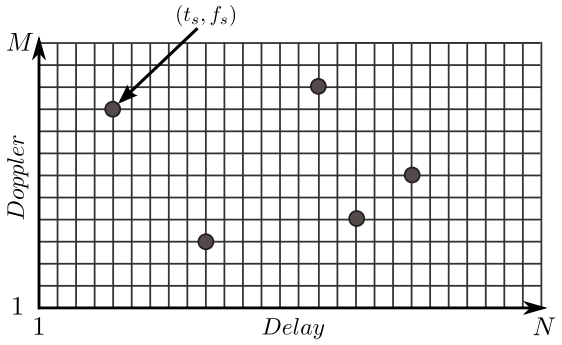

Fig. 1: A quantized delay-Doppler plane with N uniform delay grids and M uniform Doppler grids

let's denote the size of the set $\mathcal{K}$ by $K = |\mathcal{K}|$. Entries of the set $\mathcal{K}$ may be chosen deterministically or randomly from the set $\mathcal{I}$. Practically, the Fourier coefficients in the radar receiver may be acquired using different hardwares, such as sampling kernels [20], [21] or multichannel sampling schemes [22]–[24]. Let us denote the incomplete measurements obtained from the p^{th} PRI by a $K \times 1$ vector $\mathbf{y}_p = [\bar{Y}_p[\kappa_1], \bar{Y}_p[\kappa_2], \ldots, \bar{Y}_p[\kappa_K]]^T$, where κ_i for $i = 1, 2, \ldots, K$ denotes the i^{th} element of the set $\mathcal{K}$ and we define $\bar{Y}_p[k] = \tau Y_p[k]/H(\omega_k)$. The measurement matrix $\mathbf{Y} = [\mathbf{y}_0, \mathbf{y}_1, \ldots, \mathbf{y}_{P-1}]$ is constructed by collecting the measurement vectors $\mathbf{y}_p$ for $p = 0, 1, \ldots, P-1$,

$$\mathbf{Y} = \begin{bmatrix} \bar{Y}_0[\kappa_1] & \bar{Y}_1[\kappa_1] & \cdots & \bar{Y}_{P-1}[\kappa_1] \\ \bar{Y}_0[\kappa_2] & \bar{Y}_1[\kappa_2] & \cdots & \bar{Y}_{P-1}[\kappa_2] \\ \vdots & \vdots & \ddots & \vdots \\ \bar{Y}_0[\kappa_K] & \bar{Y}_1[\kappa_K] & \cdots & \bar{Y}_{P-1}[\kappa_K] \end{bmatrix}. \tag{7}$$

Next, we need a mathematical relation between the low-rate measurement samples $\mathbf{Y}$ and the sparse delay-Doppler plane of the radar. To do this, first consider a quantized delay-Doppler plane with N uniform delay grids over $[0, \tau)$ and M uniform Doppler frequency grids over $[-1/2\tau, 1/2\tau)$, as illustrated in Fig. 1. So the n^{th} delay grid indicates the delay of $t_n = \frac{(n-1)\tau}{N}$ and the m^{th} Doppler frequency grid represents the Doppler frequency of $f_m = -\frac{1}{2\tau} + \frac{m-1}{M\tau}$. We denote this quantized delay-Doppler plane by an $M \times N$ matrix $\mathbf{X}$, which has only S non-zero elements. Here, we consider several approaches that relates the measurement matrix $\mathbf{Y}$ to the sparse delay-Doppler plane matrix $\mathbf{X}$.

A. The Standard Models

The models proposed in [7] and [8], which we call them standard models, use a standard CS algorithm with huge dictionary-size to recover sparse targets in the delay-Doppler plain. Here, we introduce a new formulation for the standard models, which helps us develop simple models and recovery algorithms when we discuss our dictionary construction.

Consider the column vectors $\mathbf{y}$ and $\mathbf{x}$, which are constructed by concatenating all columns of the measurement matrix $\mathbf{Y}$ and sparse matrix $\mathbf{X}$, respectively. Assuming that targets lie exactly on the delay-Doppler grids, one can show (5) may be written in the matrix form

$$\mathbf{y} = (\mathbf{\Phi} \otimes \mathbf{\Psi})\mathbf{x}, \tag{8}$$

where $\otimes$ denotes the Kronecker product, vector $\mathbf{x}$ is an S-sparse vector (*i.e.* it has at most S non-zero elements), $\mathbf{\Phi} = [\Phi_{kn}]$ is a $K \times N$ matrix where $\Phi_{kn} = e^{-j\omega_k t_n}$ and $\mathbf{\Psi} = [\Psi_{pm}]$ is a $P \times M$ matrix where $\Psi_{pm} = e^{j2\pi f_m (p-1)\tau}$. We call $\mathbf{\Phi}$ and $\mathbf{\Psi}$ the delay and Doppler dictionaries, respectively.

Let denote the Kronecker product of the delay and Doppler dictionaries by $\mathbf{A} = \mathbf{\Phi} \otimes \mathbf{\Psi}$. Then, we can almost always recover the sparse vector $\mathbf{x}$ by solving the following optimization problem [25]

$$\min_{\mathbf{x}} \|\mathbf{x}\|_1 \quad \text{subject to} \quad \mathbf{y} = \mathbf{A}\mathbf{x}, \tag{9}$$

assuming that S is small enough compared to the number of measurements.

Note that in reality, our measurements are contaminated by noise. In this case, instead of solving the optimization (9), we can solve the following optimization

$$\min_{\mathbf{x}} \|\mathbf{x}\|_1 \quad \text{subject to} \quad \|\mathbf{y} - \mathbf{A}\mathbf{x}\|_{\mathbf{2}} \leqslant \varepsilon, \tag{10}$$

where ε is a bound on the noise magnitude chosen appropriately [25].

Numerous tools and algorithms in convex optimization [26] may be employed to solve (9) and (10). Greedy algorithms are an alternative approach to obtain the sparse vector $\mathbf{x}$. These algorithms are iterative in nature and select columns of matrix $\mathbf{A}$ according to their correlation with the measurement $\mathbf{y}$. There are several greedy algorithms proposed for the sparse recovery. The orthogonal matching pursuit (OMP) [27] and the iterative hard thresholding (IHT) [28] are the two simple and well-known greedy methods commonly used in the most CS applications. The setting that uses only the sparsity of the unknown vector to regularize the problem of finding $\mathbf{x}$ in (8) is called the standard CS [6].

When $\mathbf{x}$ is recovered, it is easy to obtain the delay-Doppler matrix $\mathbf{X}$, where the indices of its non-zero elements show indices of the delay and Doppler grids. Note that each non-zero element of $\mathbf{X}$ is a complex number that corresponds to one target and its value is equal to the attenuation factor a_s of that target. However, in real world scenarios, targets do not lie exactly on the delay-Doppler grid. Due to this fact, even in the noiseless setting, CS algorithms recover the values of $\mathbf{X}$ with different leakage attenuation based on the position of the targets. This leakage effect can be reduced by increasing the number of delay and Doppler grids in high resolution radars.

Unfortunately, the standard model uses a dictionary with the size of $PK \times MN$, which is proportional to the number of delay-Doppler grid size. The huge dictionary-size in high resolution radars results in recovery algorithms with very high computational complexity. In the following, we develop two models by breaking the huge dictionary of the standard model to smaller dictionaries. This reduction helps us employing recovery algorithms with much lower computational complexity.

B. The Proposed Structured Method

In addition to sparsity, we sometimes have extra knowledge about the structure of the measured signal. Structured CS uses this knowledge in order to reduce the sampling rate or improve the recovery performance compared to the standard CS [6].

The proposed structured method uses a similar procedure as the model used in [10]. However, our method uses a CS-dictionary to recover the delay-Doppler plain, while the proposed method in [10] uses complicated spectral estimation tools for recovery.

To model radar measurements based on structured CS, first, we recover the delays of targets. In this case, the measurements corresponding to the p^{th} PRI can be written as

$$\mathbf{y}_p = \mathbf{\Phi}\mathbf{b}_p, \tag{11}$$

where $\mathbf{\Phi}$ is the delay dictionary and $\mathbf{b}_p$ is an S-sparse vector with non-zero elements at indices of the delay grids corresponding to target delays. One can easily show that the non-zero element of $\mathbf{b}_p$ resulting from the s^{th} target have the value proportional to $e^{j2\pi f_s(p-1)\tau}$. Furthermore, all sparse vectors $\{\mathbf{b}_p\}_{p=1}^{P}$ have the same support, because we assume that the unknown parameters of the received signal are constant during each CPI.

Consequently, the multiple measurements of radar can be modeled as

$$\mathbf{Y} = \mathbf{\Phi}\mathbf{B}, \tag{12}$$

where $\mathbf{Y}$ is the measurement matrix, defined in (7), and $\mathbf{B} = [\mathbf{b}_1, \mathbf{b}_2, \dots, \mathbf{b}_P]$ denotes an $N \times P$ matrix where the p^{th} column of $\mathbf{B}$ is equal to $\mathbf{b}_p$.

The analogue of standard CS recovery problem in the multiple measurements case is [29], [30]

$$\min_{\mathbf{B}} \|\mathbf{B}\|_{1,q} \quad s.t. \quad \mathbf{Y} = \mathbf{\Phi}\mathbf{B}, \tag{13}$$

for some $q \geqslant 1$ ($q = 1, 2$ and ∞ have been used in literature), where we define $\|\cdot\|_{i,q}$ as

$$\|\mathbf{B}\|_{i,q} = \left(\sum_{n=1}^{N} \|\tilde{\mathbf{b}}_n\|_i^q \right)^{\frac{1}{q}}. \tag{14}$$

Similar to standard CS, there are various algorithms, based on the greedy pursuit [31], [32] and convex optimization [33], that use the joint sparsity knowledge of the measured signal to recover the matrix $\mathbf{B}$ from the multiple measurement vectors (MMV). After successful recovery of the delays of the targets, we keep the delay indices of targets on the delay grid in the set $\mathbf{\Omega}$. Next, Doppler frequencies of each target can be estimated by solving the following S low complexity standard CS problems:

$$\tilde{\mathbf{b}}_n = \mathbf{\Psi}\mathbf{x}_n, \quad n \in \mathbf{\Omega}, \tag{15}$$

where $\tilde{\mathbf{b}}_n$ denotes the n^{th} column of $\mathbf{B}^T$, $\mathbf{\Psi}$ is the Doppler dictionary and $\mathbf{x}_n$ is the n^{th} column of the delay-Doppler matrix $\mathbf{X}$.

An alternative approach to estimate the Doppler frequency corresponding to $\tilde{\mathbf{b}}_n$ is using FFT, similar to the conventional Nyquist processing. It is enough to find the peak of FFT($\tilde{\mathbf{b}}_n$) and the frequency corresponds to this peak. The above proposed algorithm may be utilized to recover the delay-Doppler matrix $\mathbf{X}$, by breaking the solving procedure of the previous standard model, given in (9), with the dictionary size of $PK \times MN$ to two steps. Step one is solving one simultaneous delay recovery problem, given in (12), with the dictionary size of $K \times N$, and step two includes $|\mathbf{\Omega}|$ (the number of recovered delays) standard Doppler recovery problems, given in (15), with the dictionary size of $P \times M$. We can see that the complexity of solving the introduced subproblems for the recovery of delay-Doppler plane is much lower than the complexity of solving the original standard model.

The problem of delay-Doppler recovery may be solved via the Doppler focusing approach [11] by solving M standard recovery problem with the dictionary size of $K \times N$. We discuss this method in the next subsection.

C. Doppler Focusing

Similar to the proposed algorithm in Section II-B, Doppler focusing is also a recovery approach with low computational complexity, which has recently been proposed for sub-Nyquist radars [11]. Actually, this approach first recovers the Doppler frequencies of the targets by using FFT (or filter bank with non-uniform Doppler grids) and later finds the delays of the targets. In Doppler focusing the order of recovering delays and Doppler frequencies are reversed compared to the proposed method in Section II-B.

In the Doppler focusing, first, we calculate M focused measurements by filtering measurements of P pulses around a Doppler grid as follows:

$$d_m[k] = \sum_{p=0}^{P-1} \bar{Y}_p[k] e^{-jf_m p\tau}, \quad k \in \mathcal{K},\ 1 \leqslant m \leqslant M, \tag{16}$$

where $d_m[k]$ denotes the focused Fourier coefficient with index k, around the m^{th} Doppler grid with frequency of f_m. Note that, if Doppler grids are chosen uniformly, then (16) is actually the definition of the discrete Fourier transform (DFT) of length P. It is shown that using focused measurements improves SNR proportional to the number of pulses P [11]. Let vector $\mathbf{d}_m$ denote the focused measurement vector, where k^{th} element of $\mathbf{d}_m$ is $d_m[k]$. We can recover delays of targets for each focused area by solving the standard CS problems as below

$$\mathbf{d}_m = \mathbf{\Phi}\tilde{\mathbf{x}}_m, \quad 1 \leqslant m \leqslant M, \tag{17}$$

where $\tilde{\mathbf{x}}_m$ denotes the m^{th} column of $\mathbf{X}^T$.

To compare, we summarize the number of problems and dimension of each problem for different measurement models in Table I.

TABLE I: Comparison of dimensions and number of problems for each model

Measurements Model	Number of Problems	Dictionary	Dimensions
Standard Model	1	$\mathbf{\Phi} \otimes \mathbf{\Psi}$	$KP \times NM$
Structured Model	1	$\mathbf{\Phi}$	$K \times N$
	$\lvert\mathbf{\Omega}\rvert$	$\mathbf{\Psi}$	$P \times M$
Doppler Focusing (DF)	M	$\mathbf{\Phi}$	$K \times N$

In the next section, we investigate the necessary conditions on the measurement dictionaries to guarantee uniqueness of recovery.

III. Dictionary Coherence Analysis

The CS-dictionary should be designed such that the number of measurements is reduced as much as possible, and the uniqueness of measurement for any particular signal $\mathbf{x}$ is guaranteed as well. Coherence is one of the easily computable properties of $\mathbf{\Phi}$ that guarantees distinct signals $\mathbf{x}$ and $\tilde{\mathbf{x}}$, lead to different measurement vectors $\mathbf{\Phi x}$ and $\mathbf{\Phi}\tilde{\mathbf{x}}$. This property is defined as follows [34]

Definition 1. *The coherence of a dictionary $\mathbf{\Phi} = [\phi_1, \phi_2, \ldots, \phi_N]$, denoted by $\mu(\mathbf{\Phi})$, is the largest absolute inner product between any two columns ϕ_i, ϕ_j of $\mathbf{\Phi}$*

$$\mu(\mathbf{\Phi}) = \max_{1 \leqslant i < j \leqslant N} \frac{|\langle \phi_i, \phi_j \rangle|}{\|\phi_i\|_2 \|\phi_j\|_2}.$$

In the other words, the coherence is the maximum cross-correlation between normalized columns (*i.e.* atoms) of the dictionary. It has been shown that $\mu(\mathbf{\Phi})$ is lower bounded by $\sqrt{\frac{N-K}{K(N-1)}}$ [35], which is known as the *Welch bound*.

Lemma 1 gives the necessary condition on the measurement matrix $\mathbf{\Phi}$ that guarantees uniqueness of recovery.

Lemma 1. *For a matrix $\mathbf{\Phi}$, if*

$$S < \frac{1}{2}\left(1 + \frac{1}{\mu(\mathbf{\Phi})}\right), \tag{18}$$

then for each measurement vector $\mathbf{y}$ there exists at most one S-sparse signal $\mathbf{x}$ such that $\mathbf{y} = \mathbf{\Phi x}$ [36], [37].

In this section, we look for the best sampling index set $\mathcal{K}$ that minimizes coherence of the delay dictionary, without decreasing the radar resolution. By substituting values of $\omega_k = 2\pi\kappa_k/\tau$ and delay grids $t_n = (n-1)\tau/N$ in the delay dictionary $\mathbf{\Phi}$, defined in (8), we may rewrite the dictionary as

$$\mathbf{\Phi} = \begin{pmatrix} 1 & e^{-j\frac{2\pi}{N}\kappa_1} & \ldots & e^{-j\frac{2\pi}{N}\kappa_1(N-1)} \\ 1 & e^{-j\frac{2\pi}{N}\kappa_2} & \ldots & e^{-j\frac{2\pi}{N}\kappa_2(N-1)} \\ \vdots & \vdots & \ddots & \vdots \\ 1 & e^{-j\frac{2\pi}{N}\kappa_K} & \ldots & e^{-j\frac{2\pi}{N}\kappa_K(N-1)} \end{pmatrix}, \tag{19}$$

where κ_k denotes the k^{th} element of the set $\mathcal{K}$ and N is the number of delay grids.

If we denote the normalized cross-correlation between the ℓ^{th} and the $(\ell+u)^{\text{th}}$ columns of the dictionary $\mathbf{\Phi}$ by $\mu(u)$, the coherence of $\mathbf{\Phi}$, according to Definition 1, is given by

$$\mu(\mathbf{\Phi}) = \max_{1 \leqslant u \leqslant N} \mu(u) = \max_{1 \leqslant u \leqslant N} \frac{1}{K}\left|\sum_{k=1}^{K} e^{-j2\pi\frac{u}{N}\kappa_k}\right|. \tag{20}$$

As mentioned in the previous section, the entries of the set $\mathcal{K}$ may be chosen deterministically or randomly from the set of the all Fourier indices $\mathcal{I}$.

Here we discuss different sampling schemes of the set $\mathcal{I}$:

A. Consecutive Sampling

The simplest sampling scheme uses a sampling index set $\mathcal{K}$ which the elements of $\mathcal{K}$ are consecutive elements of $\mathcal{I}$. It is obvious that in this case (20) is the summation of a geometric sequence, which is equal to

$$\mu(\mathbf{\Phi}) = \max_{1 \leqslant u \leqslant N} \mu(u) = \max_{1 \leqslant u \leqslant N} \frac{1}{K}\left|\frac{\sin(\pi u K/N)}{\sin(\pi u/N)}\right|. \tag{21}$$

We conclude from (21) that

- The adjacent columns in the delay dictionary, related to adjacent delay grids, have the most correlation and $\mu(u)$ maximizes for $u = 1$.
- Increasing the number of grids can make adjacent atoms to become more correlated.
- It is possible to design a dictionary with orthogonal columns, if and only if $N = K$. In this case, the number of samples determines the grid resolution.

This means that the consecutive sampling does not have any advantage over the Nyquist sampling, because the radar resolution is proportional to the sampling rate. This diminishes the main goal of CS, *i.e.* reducing the sampling rate without losing resolution. Furthermore, one can limit the bandwidth of the received signal with an appropriate filter and use Nyquist processing to achieve the same performance with a recovery algorithm that has a lower computational complexity. This is the main problem of consecutive sampling that is observed in [11] and [10].

B. Random Sampling

In this case, the measurements of each pulse is acquired by randomly choosing the entries of the set $\mathcal{K}$ from the set $\mathcal{I}$. Random sampling is a favorite scheme in the CS literature as it improves the mean coherence of the dictionary. It is shown that random partial Fourier matrices, with $O(S\log^5 N)$ measurements, guarantee unique recovery of an S-sparse vector with high probability [38]. However, in some radar applications, it is very important to have a reliable result in the worst case for each target estimation, and not have a reliable estimation on average. Moreover, random sampling requires more complex and sometimes impractical sampling hardware. So we are interested in optimal deterministic sampling schemes for CS-based radars.

C. Optimal Sampling

In order to achieve the highest possible resolution for the delay recovery and minimize the number of samples required for unique recovery, we must design $\mathbf{\Phi}$ with the minimum coherence, *i.e.* the coherence of $\mathbf{\Phi}$ should become equal to the Welch bound. This problem is formulated mathematically as

$$\text{find } \mathcal{K} \subseteq \mathcal{I} \quad s.t. \quad \mu(\mathbf{\Phi}) = \sqrt{\frac{N-K}{K(N-1)}}. \tag{22}$$

It is shown that the difference sets may be employed to create complex code-books that have coherence equal to the Welch bound [19]. This result may be extended to CS theory and we can prove that the coherence of the delay dictionary, which is constructed via the difference set $\mathcal{K}$ is equal to the Welch bound. Before continuing, let us define a difference set.

Definition 2. *A subset $\mathcal{K} = \{\kappa_1, \kappa_2, \ldots, \kappa_K\}$ of $\mathbb{Z}_N$ is called an (N, K, λ) difference set if set of the $K(K-1)$ modulo N differences of the form*

$$\mathcal{D}_N = \bigcup_{k=1}^{K} \bigcup_{\substack{l=1 \\ l \neq k}}^{K} \Big\{ (\kappa_k - \kappa_l) \ mod \ N \Big\} \tag{23}$$

contains every non-zero values of $\mathbb{Z}_N$ exactly λ times.

According to this definition, the three parameters (N, K, λ) are not independent and they satisfy

$$\lambda(N-1) = K(K-1). \tag{24}$$

Theorem 1. *The coherence of a $K \times N$ delay dictionary $\mathbf{\Phi}$, defined in* (19)*, is equal to the Welch bound if the sampling index set $\mathcal{K}$ is an (N, K, λ) difference set.*

Proof: One solution to the problem (22) is obtained by considering a special case that all atoms have the same cross-correlation with each others. In other words, we find atoms of a dictionary such that

$$\text{find } \mathcal{K} \subseteq \mathcal{I} \quad s.t. \quad \mu(u) = \sqrt{\frac{N-K}{K(N-1)}}, \ 1 \leqslant u \leqslant N. \tag{25}$$

We follow the steps of [19] to show that the coherence of $\mathbf{\Phi}$ is equal to the Welch bound. From (20), we have

$$\begin{aligned} \mu^2(u) &= \frac{1}{K^2} \left(\sum_{k=1}^{K} e^{-j2\pi u \kappa_k / N} \right) \left(\sum_{l=1}^{K} e^{j2\pi u \kappa_l / N} \right) \\ &= \frac{1}{K} + \frac{1}{K^2} \sum_{k=1}^{K} \sum_{\substack{l=1 \\ l \neq k}}^{K} e^{j2\pi u(\kappa_l - \kappa_k)/N} \\ &= \frac{N-K}{K(N-1)} + \frac{K-1}{K(N-1)} \\ &\quad + \frac{1}{K^2} \sum_{k=1}^{K} \sum_{\substack{l=1 \\ l \neq k}}^{K} e^{j2\pi u(\kappa_l - \kappa_k)/N}. \end{aligned} \tag{26}$$

By defining

$$z[u] \triangleq K^2 . \left(\mu^2(u) - \frac{N-K}{K(N-1)} \right), \tag{27}$$

and

$$\lambda_0 \triangleq \frac{K(K-1)}{N-1},$$

we can rewrite (26) as

$$z[u] = \lambda_0 + \sum_{k=1}^{K} \sum_{\substack{l=1 \\ l \neq k}}^{K} e^{j2\pi u(\kappa_l - \kappa_k)/N}. \tag{28}$$

Consider the set $\mathcal{D}_N = \{\kappa_l - \kappa_k \mid 1 \leqslant k, l \leqslant K, k \neq l\}$. Assume that number of elements in $\mathcal{D}_N$ with the value d is equal to λ_d, for $d = 1, ..., N-1$. Then, (28) can be written as

$$z[u] = \sum_{d=0}^{N-1} \lambda_d \, e^{j2\pi u d/N}. \tag{29}$$

Notice that in (29) the sequence $\{z[u] \ : \ 1 \leqslant u \leqslant N\}$ is the inverse discrete Fourier transform (IDFT) of the sequence $\{\lambda_d \ : \ 1 \leqslant d \leqslant N\}$. According to (27) and (29), it can be seen that the set $\mathcal{K}$ is the solution of (25) if

$$z[0] = \frac{K(K-1)N}{N-1}, \text{ and } z[1] = 0, z[2] = 0, \ldots, z[N-1] = 0, \tag{30}$$

which leads to

$$\lambda_0 = \lambda_1 = \ldots = \lambda_{N-1} = \frac{K(K-1)}{(N-1)}. \tag{31}$$

This is due to the fact that the delta function and the constant value function are a Fourier transform pair. This means that, all elements of the set $\mathcal{D}_N$ are repeated exactly $\lambda = \frac{K(K-1)}{(N-1)}$ times. So, the only solution of the problem (25) according to (24) must be an (N, K, λ) difference set. ■

We can extend the result of this theorem to CS-based radar models by following lemmas.

Lemma 2. *Consider a CS-based radar with the structured measurement model (introduced in Section II-B) and sampling index set $\mathcal{K}$, where $\mathcal{K} \subseteq \mathcal{I}$ and the set $\mathcal{I}$ is defined in* (6)*. If $\mathcal{K}$ is an (N, K, λ) difference set with $K \ll N$, then CS algorithms can recover at most $\lfloor \frac{1}{2}\big(1+\sqrt{K}\big) \rfloor$ unknown delays with delay resolution of τ/N.*

Proof: In the structured model, first, we recover delays of targets by estimating the jointly sparse matrix $\mathbf{B}$ in (12) or sparse vectors $\{\mathbf{b}_p\}_{p=1}^{P}$ in (11). Considering $K \ll N$, based on Theorem 1, the coherence of the delay dictionary $\mathbf{\Phi}$ can be approximated by $\mu(\mathbf{\Phi}) \approx \frac{1}{\sqrt{K}}$. So, according to Lemma 1, we can uniquely recover S-sparse vectors with sparsity level of

$$S < \frac{1}{2}\big(1+\sqrt{K}\big) \approx O(\sqrt{K}), \tag{32}$$

using appropriate CS algorithms. The delay dictionary includes highly incoherent atoms, which are related to delay grids. Therefore, the delay resolution of the recovered unique S-sparse vector is determined by the delay grids resolution, which is τ/N. Note that the number of delay grids N is determined by the order of the difference set and it is bounded by $N \leqslant \tau B_h$, because $\mathcal{K} \subseteq \mathcal{I}$ and according to (6) we have $|\mathcal{I}| = \tau B_h$. ■

Lemma 3. *(Modified Doppler focusing) Consider a CS-based radar with the Doppler focusing model (introduced in Section II-C) and sampling index set $\mathcal{K}$, where $\mathcal{K} \subseteq \mathcal{I}$ and the set $\mathcal{I}$ is defined in* (6)*. If $\mathcal{K}$ is an (N, K, λ) difference set with $K \ll N$, then CS algorithms can recover at most $\lfloor \frac{P}{2}\big(1+\sqrt{K}\big) \rfloor$ targets with the delay resolution of τ/N.*

Proof: The Doppler focusing approach, first, separates Doppler frequencies of targets using an appropriate filter bank. So, the Doppler resolution for a uniform Doppler grid is determined similar to a conventional Doppler recovery using FFT, *i.e.* $1/P\tau$ [1]. According to Theorem 1, for all separated Doppler frequencies we can uniquely recover $\tilde{\mathbf{x}}_m$ in (17) with the sparsity level of at most $\lfloor \frac{1}{2}\big(1+\sqrt{K}\big) \rfloor$. Therefore, all the delay-Doppler plain can be recovered with the sparsity level of at most $\lfloor \frac{P}{2}\big(1+\sqrt{K}\big) \rfloor$. Similar to Lemma 2, the delay

resolution is τ/N, because these models use the same delay dictionary $\mathbf{\Phi}$. ■

The search for finding new difference sets is an active area of research. However, we can find some of the well studied difference sets in [12] and [13]. Also a comprehensive repository of difference sets is available in [39]. For illustration purposes, we list several useful difference sets for high resolution CS-based radars in Tabel II. It is more efficient, if we use equivalent difference sets that have values around zero as listed in third column of Table II. Thus, the resulting indices can conform with the Fourier coefficients which are located around zero. We call the sampling scheme based on these equivalent difference sets *DS-sampling*. To obtain an equivalent difference set we can replace any element κ of an (N, K, λ) difference set by $\kappa + kN$, where k is an arbitrary integer number, because based on (23) all differences are calculated modulo N.

TABLE II: Examples of Appropriate Difference Sets for CS-based radars.

(N, K, λ)	Difference Set	DS-sampling indices
$(91, 10, 1)$	{0, 1, 3, 9, 27, 49, 56, 61, 77, 81}	{-42, -35, -30, -14, -10, 0, 1, 3, 9, 27}
$(993, 32, 1)$	{0, 1, 33, 86, 90, 132, 148, 168, 191, 213, 241, 251, 260, 262, 265, 446, 490, 507, 586, 615, 650, 656, 663, 690, 774, 792, 800, 872, 887, 926, 938, 963}	{-486, -407, -378, -343, -337, -330, -303, -219, -193, -121, -106, -67, -55, -30, 0, 1, 33, 86, 90, 132, 148, 168, 191, 213, 241, 251, 260, 262, 265, 446, 490}
(2863,54,1)	{0, 1, 18, 90, 101, 354, 429, 490, 514, 612, 620, 622, 671, 731, 753, 797, 809, 849, 911, 1054, 1074, 1083, 1087, 1171, 1178, 1199, 1236, 1306, 1387, 1458, 1622, 1637, 1669, 1672, 1714, 1837, 1843, 1868, 1873, 1916, 1942, 1983, 2010, 2029, 2063, 2086, 2149, 2213, 2347, 2361, 2516, 2555, 2571, 2609}	{-1405, -1241, -1226, -1194, -1191, -1149, -1026, -1020, -995, -990, -947, -921, -880, -853, -834, -800, -777, -714, -650, -516, -502, -347, -308, -292, -254, 0, 1, 18, 90, 101, 354, 429, 490, 514, 612, 620, 622, 671, 731, 753, 797, 809, 849, 911, 1054, 1074, 1083, 1087, 1171, 1178, 1199, 1236, 1306, 1387}

To make it more clear, here we compare coherence of different sampling schemes numerically. Consider the case that the delay dictionary $\mathbf{\Phi}$ is constructed using $N = 2863$ uniform delay grids, and $K = 54$ indices are chosen consecutively, randomly or based on the difference set represented in the last row of Table II. The cross-correlation of two atoms correspond to two delay grids versus distance u is illustrated in Fig. 2. As we have shown analytically, increasing the number of delay grids in consecutive sampling causes more correlation between adjacent columns of the dictionary. It is obvious that random sampling decreases correlation of adjacent atoms dramatically. Finally, as expected by the result of Theorem 1, the DS-sampling causes all atoms to have cross correlations equal to the Welch bound. To compare the difference between DS-sampling and random sampling we depict histogram of coherence of the dictionary $\mathbf{\Phi}$ in Fig. 3 for 10^5 dictionary construction. It is obvious that for the same number of delay grids, the coherence of delay dictionary constructed via DS-sampling is much lower than the random dictionaries.

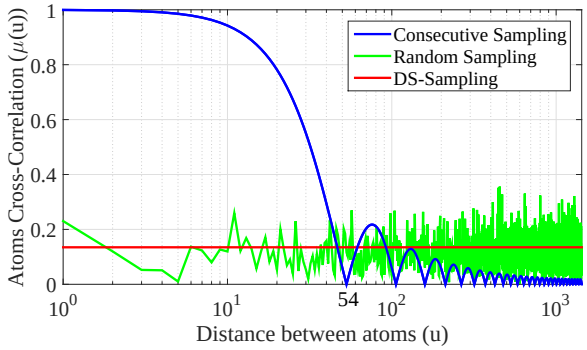

Fig. 2: Cross-correlation between atoms with distance $|u|$.

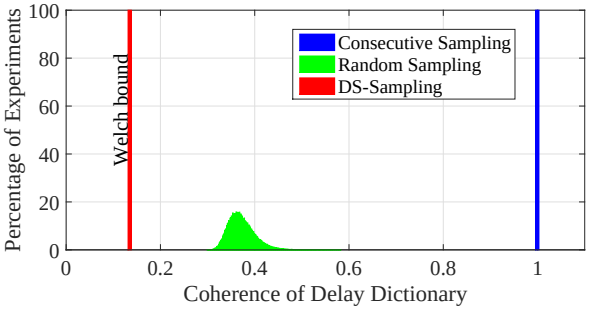

Fig. 3: Histogram of coherence of delay dictionary for different sampling schemes ($K = 54$, $N = 2863$)

All results expressed in this section may be developed for the Doppler dictionary $\mathbf{\Psi}$, defined in (15), by exchanging parameters N and K with M and P, respectively. However, normally the number of pulses P in the radar signal is much smaller in comparison to Fourier samples of each PRI. So compression in this dimension is not necessary.

IV. Recovery Algorithms

The structured method introduced in Section II-B requires a jointly sparse recovery algorithm to solve the problem (12) to obtain the joint sparse matrix $\mathbf{B}$. As mentioned previously, various algorithms are developed for jointly sparse approximation problems (see [6], [31]–[33]). After successful delay recovery, corresponding columns of the delay-Doppler matrix may be obtained by solving the standard CS problems (15). Algorithm 1 is used for the delay-Doppler recovery in the proposed structured method. In this algorithm, first, we use simultaneous orthogonal matching pursuit (SOMP) [31] to recover the joint sparse matrix $\mathbf{B}$ as well as the support of its non-zero rows (indexed by the set $\mathbf{\Omega}$). Then, the Doppler frequencies correspond to the recovered delays are determined by finding columns of the Doppler dictionary that have maximum cross-correlation with rows of $\mathbf{B}$, which are indexed by $\mathbf{\Omega}$. The stopping criterion of Algorithm 1 is set to the bound on the sparsity level, *i.e.* $\sqrt{K}$, because according to Lemma 2 we know that the number of targets must be lower than this bound to guarantee unique recovery. However, similar to any greedy algorithm, which is employed for the sparse approximation, the stopping criterion of Algorithm 1 can be

chosen to be a bound on the norm of the residual matrix, too.

Algorithm 1 Greedy Search for the Proposed Structured Model

Input: Measurement Matrix $\mathbf{Y}_{K\times P}$, Delay Dictionary $\mathbf{\Phi}_{K\times N}$, Doppler Dictionary $\mathbf{\Psi}_{P\times M}$

1: **Initialization:** $\mathbf{X}_{M\times N}=\mathbf{0}$, $\mathbf{B}_{N\times P}=\mathbf{0}, \mathbf{R}=\mathbf{Y}, \mathbf{\Omega}=\varnothing$
2: **for** $s=1$ to $\lfloor\sqrt{K}\rfloor$ **do**
3: Find an index n such that

$$n=\text{argmax}_{j\notin\mathbf{\Omega}}\,\|\phi_j^H\mathbf{R}\|_2;$$

where ϕ_j is the j'th column of $\mathbf{\Phi}$.
4: Update the support:

$$\mathbf{\Omega}=\mathbf{\Omega}\cup\{n\};$$

5: Update the estimate:

$$\mathbf{B}_{\mathbf{\Omega}}=\mathbf{\Phi}_{\mathbf{\Omega}}^{\dagger}\mathbf{R};$$

where $\dagger$ is the Moore-Penrose pseudoinverse operator [40] and $\mathbf{\Phi}_{\mathbf{\Omega}}$ denotes the restriction of $\mathbf{\Phi}$ to the columns indexed by $\mathbf{\Omega}$.
6: Update the residual:

$$\mathbf{R}=\mathbf{Y}-\mathbf{\Phi}_{\mathbf{\Omega}}\mathbf{B}_{\mathbf{\Omega}};$$

7: **end for**
8: **for** $i=1$ to $|\mathbf{\Omega}|$ **do**
9: Find index m such that

$$m=\text{argmax}_j\,\psi_j^H\tilde{\mathbf{b}}_{\Omega_i};$$

where ψ_j is the j'th column of $\mathbf{\Psi}$ and $\tilde{\mathbf{b}}_{\Omega_i}$ denotes the i'th column of $\mathbf{B}_{\mathbf{\Omega}}^T$.
10: Estimate delay-Doppler Matrix:

$$\mathbf{x}_{\Omega_i}=\text{argmin}_{\mathbf{z}}\,\|\tilde{\mathbf{b}}_{\Omega_i}-\psi_m^{\dagger}\mathbf{z}\|_2;$$

where $\mathbf{x}_{\Omega_i}$ denotes the i'th column of $\mathbf{X}_{\mathbf{\Omega}}$.
11: **end for**

Output: Estimated Delay-Doppler Matrix $\mathbf{X}$

After recovery of the delay-Doppler matrix, targets are detected by finding local maxima of $\mathbf{X}$ (or a function of $\mathbf{X}$), which are greater than a certain threshold. Threshold adjustment has close relation to the detector structure. In this paper, we do not consider the construction of the detector. For simulation purposes, we assume that the number of targets, S, is known. Thus, by finding the S largest local maxima of $\mathbf{X}$, the delay and Doppler frequency of each target can be found.

V. DS-Frequency Coded Modulated Waveform

Pulse compression is the common signal processing technique used in radars to increase the delay resolution as well as the signal to noise ratio. This is achieved by employing modulated waveforms [41]. In Section III, we show that CS-based radars can achieve the highest possible resolution using DS-sampling. Now, we look for the appropriate modulated waveform to make CS-based radars more robust in noisy conditions. CS-based radars, which perform compressed sampling in the Fourier domain, have low recovery performance in the noisy conditions in comparison to Nyquist processing methods (see the simulation results of [10] and [11]). The reason is that the signal energy is spread throughout the radar spectrum. When we reduce the Fourier domain samples, the signal energy of unsampled spectrum is discarded. To address this problem, we should employ a waveform that focuses energy around the selected Fourier domain samples. Here, we propose a frequency coded modulated waveform, called "DS-FCM" waveform, where its energy concentrates around the DS-samples.

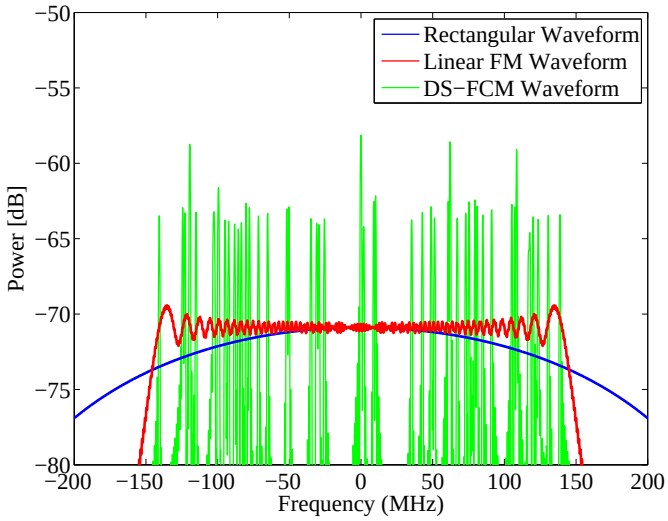

Fig. 4: Power spectrum of the Rectangular, LFM and DS-FCM waveforms. All waveforms have unit power and two-sided spectrum bandwidth of 300 MHz.

We define the DS-FCM waveform with the pulse width of T_p as

$$h(t)=\frac{1}{K}\,\text{rect}\left(\frac{t}{T_p}\right)\sum_{k\in\mathcal{K}}e^{j2\pi kt/\tau}, \tag{33}$$

where $\mathcal{K}$ is an (N,K,λ) difference set. To focus the pulse energy on DS-samples in the Fourier domain, we must increase the pulse width (*i.e.* increasing the support of signal in the time domain). So, the two-sided spectrum bandwidth of (33) is determined by its complex envelope and we may approximate B_h by the largest and smallest entries of the difference set $\mathcal{K}$ as follows

$$B_h\approx\frac{k_{\max}-k_{\min}}{\tau}, \tag{34}$$

where $k_{\max}$ and $k_{\min}$ are the largest and the smallest entries of the difference set $\mathcal{K}$, respectively.

The power spectrum of the rectangular waveform, linear frequency modulated (LFM) waveform and DS-FCM waveform, which is based on a $(2863,54,1)$ difference set, are represented in the last row of Table II, are shown in Fig. 4. All waveforms have equivalent unit power and two-sided

bandwidth of 300 MHz. It is obvious that the energy of DS-FCM waveform is focused around the Fourier samples rather than the entire spectrum.

VI. Simulation Results

The performance of the proposed sub-Nyquist sampling and processing methods have been evaluated by means of simulation. To compare, results obtained from the conventional Nyquist processing and Doppler focusing approach with the consecutive sampling are also presented. The following specifications and parameters are used in the simulations:

- Radar PRI[2]: $\tau = 10\ \mu s$
- Receiver bandwidth: $B_h = 300$ MHz (two-sided spectrum bandwidth of the pulse $h(t)$)
- Number of pulses: $P = 20$
- Nyquist sampling rate: $B_h = 300$ MSPS $= 3000$ samples per PRI
- 128-point FFT is used in Nyquist processing and the corresponding Doppler dictionary in sub-Nyquist methods include 128 Doppler grids.
- A rectangular waveform with the two-sided spectrum bandwidth of B_h is used for the Nyquist processing.
- Sub-Nyquist methods use DS-FCM waveform, unless it is specified.
- DS-sampling and DS-FCM waveform, which are used in the sub-Nyquist methods, are based on the $(2863, 54, 1)$ difference set, given in the last row of Table II. This sampling scheme uses only 54 samples per PRI, which is less than 2% of the Nyquist samples.
- Number of targets $S = 5$, unless it is specified.
- Target delays and Doppler frequencies are distributed uniformly at random over the unambiguous delay-Doppler region and the attenuation factors associated with each target is taken to have a unit amplitude and a random phase.

We consider the case that all received signals contaminated by zero mean complex additive white Gaussian noise (AWGN) with variance σ_w^2. In this setting, the signal to noise ratio (SNR) of the received signal from the s^{th} target is

$$\text{SNR}_s = \frac{\frac{1}{T_p}\int_0^{T_p} |a_s h(t)|^2 \,\mathrm{d}t}{\sigma_w^2 B_h}, \tag{35}$$

where T_p is the pulse width of the transmitted signal. In the numerical simulations, where an analog signal is modeled with its high rate sampled discrete equivalent, the SNR of the s^{th} target can be calculated as

$$\text{SNR}_s = \frac{\|a_s \mathbf{h}\|_2^2}{L\sigma_w^2}, \tag{36}$$

where the L-length vector $\mathbf{h}$ is the discrete equivalent of the continuous signal $h(t)$. Notice that, if the entries of $\mathbf{h}$ are the Nyquist samples of $h(t)$, then $L = \lfloor T_p B_h \rfloor$.

The conventional Nyquist processing delay and Doppler frequency resolution (Nyquist bins) are defined as $\delta_t = 1/B_h$ and $\delta_f = 1/P\tau$, respectively. Since we are interested in comparison of sub-Nyquist methods with the conventional Nyquist processing, the following performance metrics based on the Nyquist bins will be useful.

1) **Probability of Detection:** A "*true detection*" is defined as a delay-Doppler estimation with the error less than Nyquist bins. In other words, we have a true detection for the s^{th} target if its estimated delay and Doppler frequency satisfy

$$|\hat{t}_s - t_s| < \delta_t \quad \text{and} \quad |\hat{f}_s - f_s| < \delta_f,$$

where t_s and $\hat{t}_s$ denote the true and the estimated delay of the s^{th} target, respectively. Similarly, the true and the estimated Doppler frequency of the s^{th} target are denoted by f_s and $\hat{f}_s$, respectively.

2) **Normalized RMS Error:** For all true detections, the normalized RMS error of estimated delays and Doppler frequencies are defined as

$$e_t \overset{\text{def}}{=} \sqrt{\frac{1}{T}\sum_{s=1}^{T}\left(\frac{\hat{t}_s - t_s}{\delta_t}\right)^2}$$

and

$$e_f \overset{\text{def}}{=} \sqrt{\frac{1}{T}\sum_{s=1}^{T}\left(\frac{\hat{f}_s - f_s}{\delta_f}\right)^2},$$

respectively, where T denotes the total number of true detections.

3) **Probability of Separate Detection:** We define "*Separate Detection*" as detection of two close targets with the delay and Doppler errors less than half of their true delay and Doppler frequency spacing in the delay-Doppler plain, respectively. To be more specific, let $t_{ij} = |t_i - t_j|$ and $f_{ij} = |f_i - f_j|$ denote the true delay and Doppler frequency spacing of the i^{th} and the j^{th} targets, respectively. If the estimated delays and Doppler frequencies satisfy

$$\forall s \in \{i, j\} : |\hat{t}_s - t_s| < \frac{t_{ij}}{2} \quad \text{and} \quad |\hat{f}_s - f_s| < \frac{f_{ij}}{2},$$

then we say these two targets are detected separately.

A. Recovery Performance

We first study the effect of radar waveform, the number of samples and radar measurement model on recovery performance in the noisy settings. The results of this experiment are shown in Fig. 5, which plots the probability of detection as a function of SNR. It can be seen that the recovery performance of sub-Nyquist methods degrades with reduction of sampling rate in radars with rectangular waveform. However, this performance degradation is compensated using modulated waveform that focuses energy around the sub-Nyquist samples. As can be seen, using DS-FCM waveform combined with DS-sampling considerably improves the performance of CS-based radar. It is clear that the modified-DF approach has better detection performance than other methods for SNRs below -12 dB while the structured method have better performance for

[2]This parameter is limited by the simulation running time and the availbale computer physical memory. We use this value similar to [11] for a fair comparison.

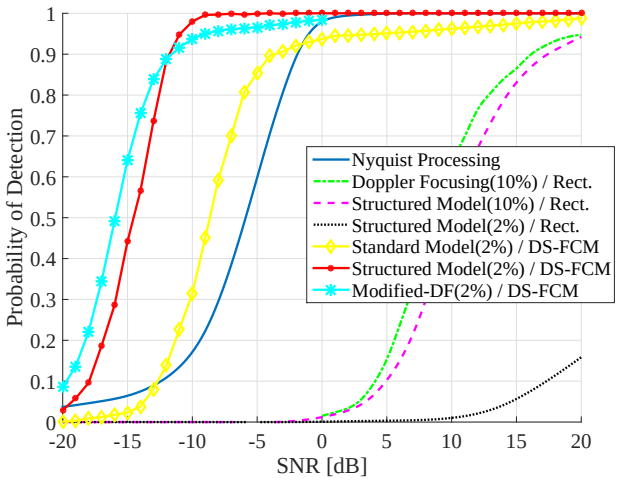

Fig. 5: Probability of detection for the conventional Nyquist processing and sub-Nyquist processing methods based on standard model, structured model, Doppler focusing (DF) approach [11], and modified-DF. Sub-Nyquist sample rate is 2% and 10% of Nyquist rate.

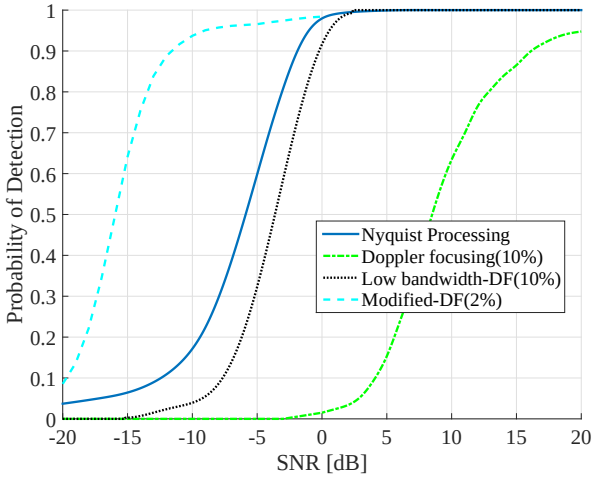

Fig. 6: Probability of detection versus SNR for different Doppler focusing approaches. Low bandwidth-DF uses a waveform with 30 MHz bandwidth, while other three methods use 300 MHz waveforms.

higher SNRs. The standard model leads to lower performance, because this method only uses sparsity of targets while two other method use joint sparsity and focused measurements to improve recovery performance. Furthermore, standard model uses a huge dictionary including $366,464$ atoms and the processor must perform a heavy combinational search over these atoms to find all targets.

The performance of Doppler focusing approach [11], which uses consecutive sampling and rectangular waveform, is much less than the conventional Nyquist processing method. Moreover, increasing bandwidth of radar waveform decrease energy of each Fourier samples. To solve this problem, the authors of [11] pass the signal through a low pass filter and readjust amplitude of the resultant signal so that the target SNR remains constant (see Fig. 8. of [11] and its comments). In the other word, it is proposed that only a waveform with

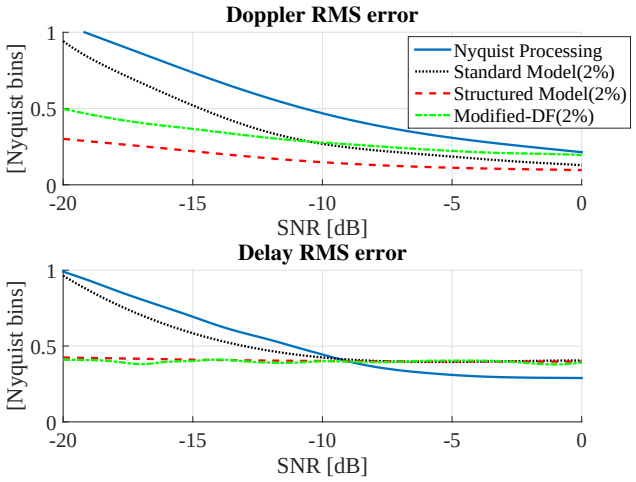

Fig. 7: Normalized RMS error of delay and Doppler frequency recovery.

reduced bandwidth, proportional to sample rate reduction, be transmitted. One can show that such assumption leads to less radar resolution. By the way, we compare all Doppler focusing approaches with the Nyquist processing in Fig. 6. It can be seen that performance of low bandwidth-DF is increased in comparison to Doppler focusing with original bandwidth waveform.

The normalized RMS error of delay and Doppler frequency estimation for high performance recovery methods are illustrated in Fig. 7. It can be seen that the structured model has less RMS error than others in Doppler recovery and RMS error of its delay recovery is similar to Modified-DF.

Recovery algorithms of sub-Nyquist methods are more complicated than the conventional Nyquist processing. However, low computational complexity algorithms can achieve faster recovery than the conventional processing, because sub-Nyquist methods in these simulations use only 2% of Nyquist samples. To compare the recovery speed, we list the required processing time for an "*Intel(R) Core(TM) i7 - 4790k @ 4.00GHz*" processor to perform each recovery method (see Table III). It is evident that by using the structured model we can achieve faster recovery time. Note that, the standard model requires large number of computations and consequently needs long time to perform recovery. Therefore, using the standard model is infeasible for high resolution radar applications, specially for long range radars. The processing time is proportional to the size of CS problem for each model

TABLE III: Processing times of various recovery methods.

Recovery Method	Number of Samples per PRI	Processing time
Conventional Nyquist Processing	3000	$1,293$ ms
Doppler Focusing Low bandwidth-DF	300	$6,686$ ms
Standard Model	54	$16,072$ ms
Modified-DF	54	472.8 ms
The Structured Model	54	70.3 ms

as listed in TABLE I.

B. Recovery Resolution

Recall from Section III that we prove analytically, DS-sampling scheme leads to a delay dictionary with minimum coherence. As each atom in the delay dictionary belongs to a specific delay grid, we expect to achieve the highest possible resolution, limited by difference set order in our sub-Nyquist sampling scheme. In these simulations, we use a difference set with order $N = 2863$ to create a delay dictionary with delay grid resolution of $\tau/N = 1.048 \times \delta_t$. The probability of separate detection is a good performance metric to represent the resolution of radar in terms of the ability to separate recovery of two closely spaced targets. We assume that the received signal from these two targets have the same SNR, which is high enough for the true detection. For example, based on Fig. 5 considering SNR = 5 dB for the Nyquist processing and structured model with DS-sampling is enough for the true detection of targets with high probability. In order to evaluate delay resolution, we consider the case that two close targets have Doppler frequency spacing less than or equal to a Doppler Nyquist bin such that the ability of separating two targets using different Doppler frequencies can not affect the delay resolution. As illustrated in Fig. 8, sub-Nyquist methods using DS-sampling can achieve better delay resolution than sub-Nyquist methods with random sampling. Furthermore, we can distinguish close targets with higher probability using sub-Nyquist methods with DS-sampling, while it uses only 2% of Nyquist samples. To compare, we also represent the resolution of sub-Nyquist methods with consecutive sampling [10], [11], which uses 10% and 15% of Nyquist samples. As we expected from the discussion presented in Section III, consecutive sampling does not exploit all information about targets, specially when the targets are close together. This property of consecutive sampling contradicts with the goal of CS theory, *i.e.* sub-sampling without loosing information.

C. The Effect of Number of Pulses

Conventional Nyquist processing methods can achieve higher recovery performance in the noisy condition by increasing the number of transmitted pulses. In this experiment, we investigate the effect of increasing the number of pulses on sub-Nyquist methods. The results of this numerical experiment are reported in Fig. 9. It can easily be seen from the figure that the behavior of sub-Nyquist methods are also improved in the noisy condition by increasing the number of pulses.

D. The Effect of Number of Targets

Our final numerical experiment studies the effect of increasing the number of targets on the recovery performance. Figure 10 shows that increasing the number of targets causes degradation in the recovery performance of sub-Nyquist method. As predicted by Lemma 2 and Lemma 3, recovery performance of the Modified-DF decreases slower by an increasing number of targets in comparison to the structured model.

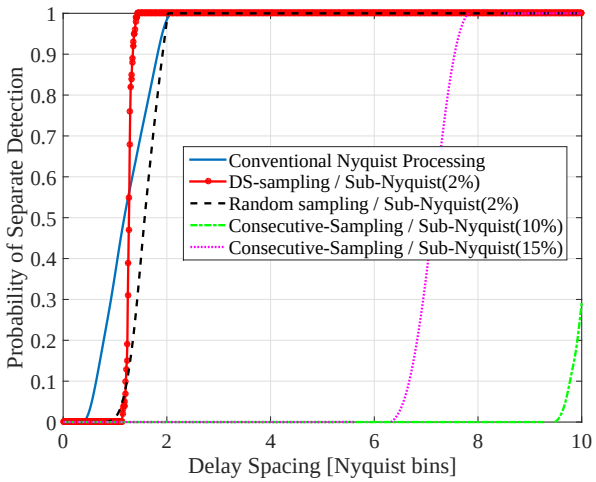

Fig. 8: Probability of separate detection of two close targets with different delay spacing on delay-Doppler plane. The sub-Nyquist methods, based on the proposed DS-sampling, random sampling and consecutive sampling [10], [11], are presented.

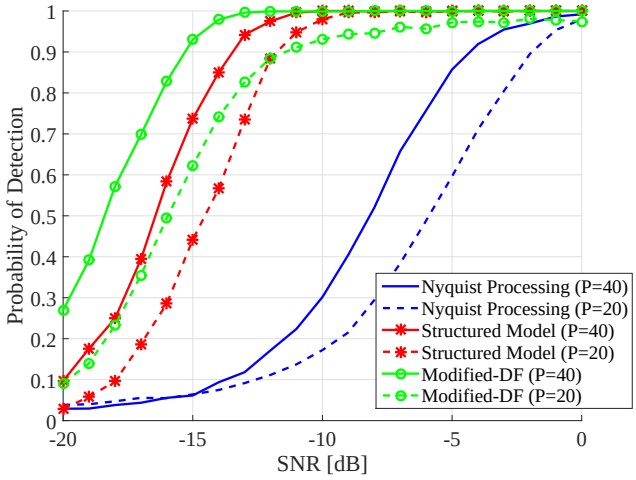

Fig. 9: Probability of detection versus SNR for different recovery methods, where the solid lines show recovery methods with $P = 40$ pulses, and the dashed lines indicate recovery methods with $P = 20$ pulses.

VII. Conclusion

This paper presents a novel sub-Nyquist sampling scheme based on difference set codes, called "DS-sampling". It is shown analytically and numerically that DS-sampling can reduce the sampling rate of wideband radars significantly without any reduction in the radar resolution. It is shown that the radar waveform has an important role in sub-Nyquist methods. We also introduce a new modulated waveform based on difference sets, called "DS-FCM" waveform, which can highly boost the recovery performance of sub-Nyquist methods in noisy conditions. The proposed structured model reduces complexity and processing time of the delay-Doppler recovery, however, its performance decreases for a large number of targets. To solve this problem, we develop a modified version of the Doppler focusing approach based on the DS-sampling and the DS-FCM waveform. Modified-DF has ability of recovering

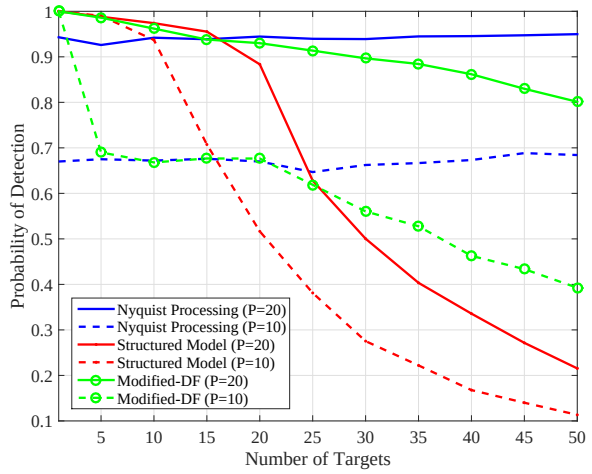

Fig. 10: Probability of detection versus the number of targets for different recovery methods, where the solid lines show recovery methods with $P = 20$ pulses, and the dashed lines indicate recovery methods with $P = 10$ pulses (SNR = 0 dB).

more targets at the cost of more processing time. Finally, we show that our sampling and processing method addresses the common problems of many CS-based radars.

REFERENCES

[1] M. Skolnik, *Introduction to radar systems*. Boston: McGraw Hill, 2003.

[2] A. J. Jerri, "The shannon sampling theorem–its various extensions and applications: A tutorial review," *Proceedings of the IEEE*, vol. 65, no. 11, pp. 1565–1596, Nov 1977.

[3] D. L. Donoho, "Compressed sensing," *IEEE Transactions on Information Theory*, vol. 52, pp. 1289–1306, 2006.

[4] E. J. Candès, "Compressive sampling," in *Proceedings of the International Congress of Mathematicians: Madrid, August 22-30, 2006: invited lectures*, 2006, pp. 1433–1452.

[5] Y. C. Eldar and G. Kutyniok, *Compressed Sensing: Theory and Applications*. Cambridge NewYork: Cambridge University Press, 2012.

[6] M. F. Duarte and Y. C. Eldar, "Structured compressed sensing: From theory to applications," *IEEE Transactions on Signal Processing*, vol. 59, no. 9, pp. 4053–4085, 2011.

[7] J. H. G. Ender, "On compressive sensing applied to radar," *Signal Processing*, vol. 90, pp. 1402–1414, 2010.

[8] M. A. Herman and T. Strohmer, "High-resolution radar via compressed sensing," *IEEE Transactions on Signal Processing*, vol. 57, pp. 2275–2284, 2009.

[9] B. Demissie and C. R. Berger, "High-resolution range-Doppler processing by coherent block-sparse estimation," *IEEE Transactions on Aerospace and Electronic Systems*, vol. 50, no. 2, pp. 843–857, Apr. 2014.

[10] W. U. Bajwa, K. Gedalyahu, and Y. C. Eldar, "Identification of Parametric Underspread Linear Systems and Super-Resolution Radar," *IEEE Transactions on Signal Processing*, vol. 59, no. 6, pp. 2548–2561, Jun. 2011.

[11] O. Bar-Ilan and Y. C. Eldar, "Sub-Nyquist radar via doppler focusing," *IEEE Transactions on Signal Processing*, vol. 62, pp. 1796–1811, 2014.

[12] A. Pott, V. Kumaran, T. Helleseth, and D. Jungnickel, *Difference sets, sequences and their correlation properties*. Dordrecht: Springer Netherlands, 2012, vol. 542.

[13] M. Hall, *Combinatorial theory*. New York Chichester: John Wiley & Sons, 1998, vol. 71.

[14] C.-S. Weng and J. Wu, "Perfect difference codes for synchronous fiber-optic CDMA communication systems," *Journal of Lightwave Technology*, vol. 19, no. 2, pp. 186–194, 2001.

[15] V. P. Ipatov, "On the Karystinos-Pados Bounds and Optimal Binary DS-CDMA Signature Ensembles," *IEEE Communications Letters*, vol. 8, no. 2, pp. 81–83, Feb. 2004.

[16] L. E. Kopilovich, "Square array antennas based on Hadamard difference sets," *IEEE Transactions on Antennas and Propagation*, vol. 56, no. 1, pp. 263–266, 2008.

[17] G. Oliveri, M. Donelli, and A. Massa, "Linear array thinning exploiting almost difference sets," *IEEE Transactions on Antennas and Propagation*, vol. 57, no. 12, pp. 3800–3812, 2009.

[18] Y. Kato and T. Morita, "Error correction circuit using difference-set cyclic code," in *Design Automation Conference, 2003. Proceedings of the ASP-DAC 2003. Asia and South Pacific*, Jan 2003, pp. 585–586.

[19] P. Xia, S. Zhou, and G. B. Giannakis, "Achieving the Welch Bound With Difference Sets," *IEEE Transactions on Information Theory*, vol. 51, no. 5, pp. 1900–1907, May 2005.

[20] R. Tur, Y. C. Eldar, and Z. Friedman, "Innovation rate sampling of pulse streams with application to ultrasound imaging," *IEEE Transactions on Signal Processing*, vol. 59, pp. 1827–1842, 2011.

[21] M. Unser, "Sampling – 50 years after Shannon," *Proceedings of the IEEE*, vol. 88, pp. 569–587, 2000.

[22] K. Gedalyahu, R. Tur, and Y. C. Eldar, "Multichannel sampling of pulse streams at the rate of innovation," *IEEE Transactions on Signal Processing*, vol. 59, pp. 1491–1504, 2011.

[23] J. Kusuma and V. K. Goyal, "Multichannel sampling of parametric signals with a successive approximation property," in *Proceedings of International Conference on Image Processing, ICIP*, 2006, pp. 1265–1268.

[24] H. Olkkonen and J. T. Olkkonen, "Measurement and Reconstruction of Impulse Train by Parallel Exponential Filters," *IEEE Signal Processing Letters*, vol. 15, pp. 241–244, 2008.

[25] E. J. Candès, J. Romberg, and T. Tao, "Robust uncertainty principles: Exact signal reconstruction from highly incomplete frequency information," *IEEE Transactions on Information Theory*, vol. 52, no. 2, pp. 489–509, 2006.

[26] S. Boyd and L. Vandenberghe, *Convex optimization*. Cambridge, UK New York: Cambridge University Press, 2004.

[27] Y. C. Pati, R. Rezaiifar, and P. S. Krishnaprasad, "Orthogonal matching pursuit: recursive function approximation with applications to wavelet decomposition," *Proceedings of 27th Asilomar Conference on Signals, Systems and Computers*, 1993.

[28] T. Blumensath and M. E. Davies, "Iterative hard thresholding for compressed sensing," *Applied and Computational Harmonic Analysis*, vol. 27, no. 3, pp. 265–274, 2009.

[29] S. F. Cotter, B. D. Rao, K. Engan, and K. Kreutz-Delgado, "Sparse solutions to linear inverse problems with multiple measurement vectors," *IEEE Transactions on Signal Processing*, vol. 53, no. 7, pp. 2477–2488, 2005.

[30] M. Fornasier and H. Rauhut, "Recovery algorithms for vector-valued data with joint sparsity constraints," *SIAM Journal on Numerical Analysis*, vol. 46, no. 2, pp. 577–613, 2008.

[31] J. A. Tropp, A. C. Gilbert, and M. J. Strauss, "Algorithms for simultaneous sparse approximation. Part I: Greedy pursuit," *Signal Processing*, vol. 86, no. 3, pp. 572–588, 2006.

[32] M. Mishali and Y. C. Eldar, "Reduce and boost: Recovering arbitrary sets of jointly sparse vectors," *IEEE Transactions on Signal Processing*, vol. 56, no. 10, pp. 4692–4702, 2008.

[33] J. A. Tropp, "Algorithms for simultaneous sparse approximation. Part II: Convex relaxation," *Signal Processing*, vol. 86, no. 3, pp. 589–602, 2006.

[34] J. Tropp and A. C. Gilbert, "Signal recovery from partial information via orthogonal matching pursuit," 2005.

[35] L. Welch, "Lower bounds on the maximum cross correlation of signals (Corresp.)," *IEEE Transactions on Information Theory*, vol. 20, 1974.

[36] D. L. Donoho and M. Elad, "Optimally sparse representation in general (nonorthogonal) dictionaries via l minimization," *Proceedings of the National Academy of Sciences of the United States of America*, vol. 100, pp. 2197–2202, 2003.

[37] J. A. Tropp, "Greed is good: Algorithmic results for sparse approximation," *IEEE Transactions on Information Theory*, vol. 50, no. 10, pp. 2231–2242, 2004.

[38] M. Rudelson and R. Vershynin, "On sparse reconstruction from Fourier and Gaussian measurements," *Communications on Pure and Applied Mathematics*, vol. 61, no. 8, pp. 1025–1045, 2008.

[39] D. Gordon (2015, Sep 6), "La Jolla Difference Set Repository." [Online]. Available: http://www.ccrwest.org/diffsets.html

[40] G. H. Golub and C. F. Van Loan, *Matrix computations*. Baltimore: Johns Hopkins University Press, 1996.

[41] N. Levanon and E. Mozeson, *Radar Signals*. Hoboken, New Jersey: John Wiley & Sons, 2004.